# Thermally assisted spatially directed pore formation in poly-dimethylsiloxane (PDMS)

A. Banait, V. Vishwakarma, L. Choobineh, and A. Jain[a)]
*Mechanical and Aerospace Engineering Department, University of Texas at Arlington, Arlington, Texas 76019, USA*

(Received 21 June 2013; accepted 20 September 2013; published online 8 October 2013)

This paper reports a method for spatially directed, self-assembled pore formation in poly-dimethylsiloxane (PDMS) that results in through-membrane pores only at desired locations. This method is based on bubble generation in uncured PDMS and subsequent bubble motion towards a hot region in a microfabricated chip containing a heater device due to thermocapillary effect. Pore formation in straight-line and semi-circular shapes is demonstrated. Coupled physics behind the pore formation and alignment process is described. Results show that the mechanism of pore formation can be controlled by changing the microheater temperature. © *2013 AIP Publishing LLC*. [http://dx.doi.org/10.1063/1.4824444]

Poly-dimethylsiloxane (PDMS) is a well-known soft polymer with applications in a wide variety of research fields.[1–3] PDMS is a particularly attractive material for miniaturized bioanalytical systems because of its biocompatibility, gas permeability, and chemical inertness.[1] More recently, PDMS has also been investigated for use as an exchange membrane for pervaporation, separation, and purification.[4–6] The flow of fluids through a PDMS membrane is particularly important for such applications. Traditionally, microchannels are molded into PDMS using a mold master produced by patterning methods such as photolithography.[2,7] Such approaches result in in-plane microchannels. Compared to in-plane microchannels, it is a lot more challenging to produce through-membrane pores in PDMS.[8] Such pores can, in principle, be produced by using a master mold containing features with very high aspect ratio or by using high aspect ratio photoresists such as SU-8.[9] However, the length of such pores is limited by the feature height on the mold, which is usually only a few tens of microns. Some past work has described the use of hydrophobic-hydrophilic interactions to engineer through-membrane pores in PDMS.[10,11] However, the pores produced in these experiments were randomly distributed, without the possibility of controlling the location of pore formation. The random distribution severely restricts the use of such porous membranes. It is very desirable to develop methods for spatially controlled pore formation in PDMS. Spatially controllable porosity can be used, for example, in selective through-membrane fluid transport only in specific locations of a bioanalytical microsystem. Such a capability may also find applications in through-membrane mass exchange for purification, separation, etc.[4–6]

This paper describes a through-membrane pore formation method based on a spatial temperature gradient imposed by a microheater device. Temperature gradient based devices have been used in the past for controlling attachment between Deoxyribonucleic acid (DNA) and glass, cellular thermotaxis, etc.[12,13] In the present work, bubbles nucleated on the glass substrate during heating of a patterned microheater are found to migrate towards the hot microheater line due to thermocapillary migration,[14] leading to self-assembly of pores in the same shape as the microheater line. Theoretical calculations and experimental velocity measurements confirm the thermocapillary nature of bubble motion. Formation of pores in a linear and semi-circular pattern is demonstrated. This capability can be extended to any other shape by manipulating the spatial temperature profile on the substrate.

Design and microfabrication of the microheater device are described next. Experiments investigating the nature of pore formation, and its dependence on temperature and other parameters are discussed. Theoretical modeling of the process is described, and calculations showing close agreement of experimental data with the theory of thermocapillary effect are presented. Experimental results indicating the existence of four distinct temperature regimes for the pore formation process are discussed.

A microheater device with a 20 $\mu$m wide and 0.1 $\mu$m thick Titanium heater is fabricated on a standard glass slide in a class-100 cleanroom using photolithography and metal deposition in a thermal evaporator system. Two types of heaters—straight-line as well as semi-circular—are fabricated. The heater is also used as a resistance-based temperature sensor. Titanium offers high temperature coefficient of resistance, ensuring good temperature measurement sensitivity. Further, titanium also has high electrical resistance, which maximizes heat generation at a given heating current. Figure 1 shows an image of the microheater device. Photolithography masks are available as supplementary material.[15]

The microheater device is calibrated in an Instec HCS620S temperature-controlled platform. Measurement of heater resistance at different temperatures between 20 °C and 150 °C results in a linear temperature dependence, with a correlation coefficient greater than 0.999. The temperature coefficient of resistance is measured to be 0.0017/°C. Calibration curve of a typical microheater device is available as a supplementary material.[15]

A finite-element thermal simulation model for the microheater device is developed. The simulation model solves the governing energy conservation equation to determine the temperature profile for a given heating current through

[a)]Author to whom correspondence should be addressed. Electronic mail: jaina@uta.edu. Tel.: +1-817-272-9338.

 

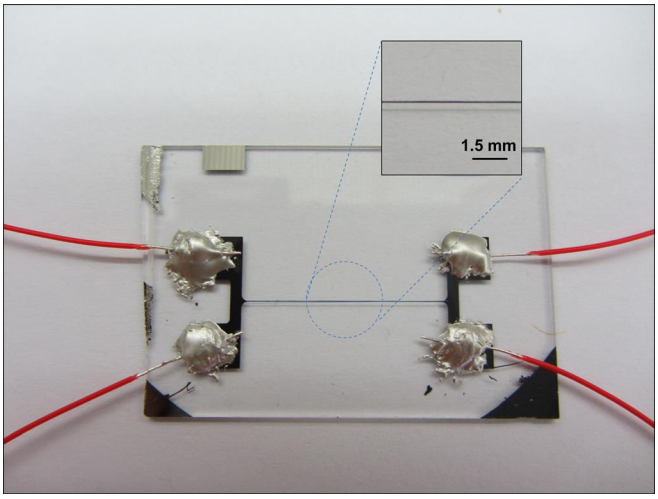


FIG. 1. Image of the microheater device used for providing the temperature gradient responsible for pore formation.

the microheater. Joule heating is assumed to occur in the microheater line, and natural convection boundary condition is assumed on other surfaces of the microheater device. Figure 2(a) shows a plot of the microheater temperature rise as a function of heating current. Experimental data exhibit the expected $I^2$ dependence and agree well with the simulation model prediction. Figure 2(b) shows the expected surface temperature as a function of distance from the microheater line for 10 mA heating current. Figure 2(b) shows that the microheater device produces a strong temperature gradient in the vicinity of the microheater line.

Past work for producing pores in PDMS used a hotplate for curing, resulting in uniform temperature, and thus pore formation all over the PDMS membrane.[10,11] The microheater device used in this work produces a spatial temperature gradient, causing bubbles to laterally migrate to the high temperature region due to thermocapillary effect, and thus making it possible to produce a pore pattern that follows the shape of the microheater line. A hydrophilic material such as polyethylene oxide (PEO) is first melted on the microheater device. The device is then treated with chlorotrimethylsilane, and uncured PDMS (Sylgard 184 with 10:1 base to hardener ratio) is poured on the chip. A pre-fabricated PDMS gasket of known dimension is carefully placed around the microheater to prevent uncured PDMS from flowing away. When the substrate is heated by passing electric current through the microheater, PEO evaporates into the PDMS, resulting in the formation of gas bubbles within the PDMS matrix. These gas bubbles rise through the uncured PDMS due to buoyancy, leaving behind a pore that extends through the PDMS thickness. The migration of bubbles towards the microheater line occurs only when a heating current through the microheater causes a spatial temperature gradient. Figures 3(a) and 3(b) show top views of pores formed in isothermal conditions using a conventional hotplate, and with the microheater line maintained at 120 °C, respectively. Typical pore diameter is around 200 $\mu$m, although sometimes two pores merge together to form a bigger one. In the first case, pores are formed in a random fashion and do not migrate laterally. In the second case, pores move towards the microheater line, resulting in a self-assembled row of pores along the microheater line. Time progression of the pore formation and migration can also be seen in Figure 4 (regime III) and in a video of the patterned pore formation process, provided as supplementary material.[15]

Experiments have identified a strong temperature-dependence of the pore formation phenomenon. Four distinct temperature regimes are observed. Figure 4 shows images of the pore formation process at different times in the four different temperature regimes. In regime I, at relatively low temperatures, not enough nucleation occurs during the curing process, resulting in no pore formation. In regime II, at slightly higher temperature, nucleation occurs, but bubbles escape the PDMS without creating pores due to the slow cure rate and low PDMS viscosity during pore formation. As the curing temperature is further increased, in regime III, a good balance between competing factors is found where the nucleation rate and PDMS viscosity are just right for pores to form and migrate laterally through the PDMS towards the microheater line. In regime III, bubbles nucleate everywhere on the substrate, but laterally move towards the high temperature microheater line due to thermocapillary effect. Once the bubbles reach the microheater, they stay locked in place. Two bubbles sometimes merge to form a single, larger pore. The lateral motion of the bubbles can be seen in the time progression for regime III shown in Figure 4, as well as in the video uploaded as supplementary material.[15] At very high temperature, in regime IV, too many gas bubbles nucleate,

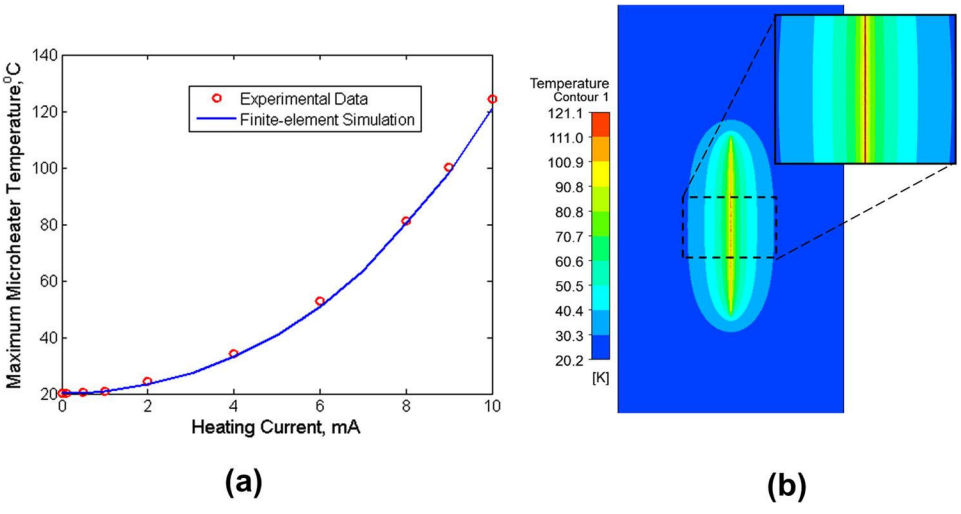


FIG. 2. (a) Maximum temperature rise in the substrate as a function of heating current; (b) Expected surface temperature profile for 10 mA heating current.

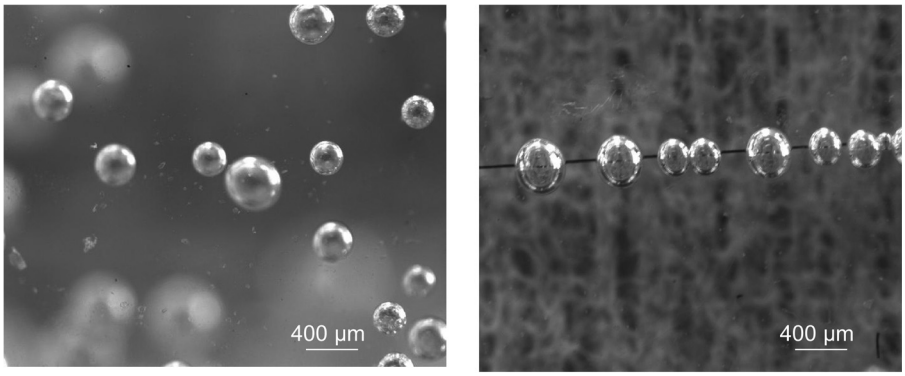


FIG. 3. Images comparing (a) randomly formed pores versus (b) pores formed in a straight-line shape using a microheater device of the same shape.

leading to overcrowding and making it difficult to obtain a good pattern of pores. Due to the rapid cure rate, bubbles also have very little time to migrate through the PDMS to the microheater before viscosity becomes high enough to lock the pores in place. The temperature range for regime III where the best pore pattern is formed is found to be 115–130 °C. Temperature ranges for other regimes are shown in Figure 4. Images (A) show the device at the start of the experiment. It takes roughly 10 s for bubbles to nucleate (images (B)). Pore motion and alignment occur over the next 50–60 s (images (C)), which is close to the time estimated for the farthest pore to travel to the microheater based on the computed thermocapillary speed.

Following the development of a linear pattern of pores along a straight microheater line, the microheater device is fabricated with semi-circular C-shaped microheaters. Following calibration, these devices are used for investigating pore formation. In this case, the pore formation in regime III follows the spatial pattern of the C-shaped microheater, resulting in a C-shaped array of pores, as shown in Figure 5(a). Figure 5(b) shows an intensity plot captured through a confocal microscope that shows the patterned pore formation for the C-shaped microheater case. This experiment demonstrates the capability of patterning pores in a desired spatial pattern. Depending on the needs of a specific mass transport application, it is possible to manipulate the spatial temperature field and thus the thermocapillary motion responsible for patterned pore formation.

We explain the observed migration of bubbles towards the high temperature microheater line using the thermocapillary effect,[14] which has been observed previously in laser-based optical trapping experiments where a spot heated by a laser has been found to attract gas bubbles.[16,17] This effect is caused by the establishment of interfacial velocity fields on both sides of the gas-liquid interface due to temperature-dependent surface tension. These velocity fields cause the bubble to roll and propel forward in the direction of increasing temperature, similar to a swimmer's forward propulsion in water.[14] The presence of a strong temperature gradient in the current experiments and the strong temperature-dependence

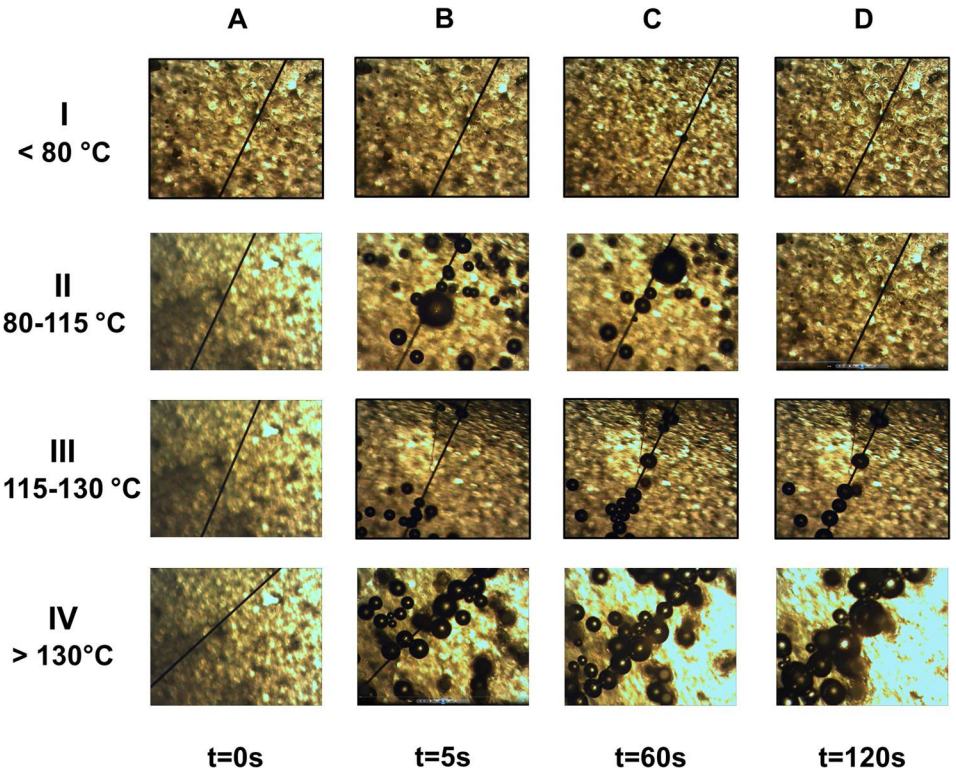


FIG. 4. Temperature regime map showing the characteristics of temperature regimes I through IV in the spatially directed pore formation process.

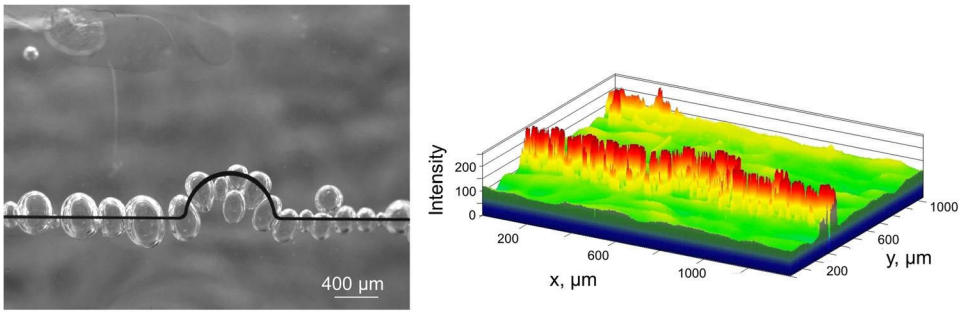


FIG. 5. (a) Image of microchannels lined up along a C-shaped microheater device, (b) intensity plot showing the patterned pore distribution.

of surface tension of PDMS[18,19] causes migration of pores towards high temperature regions due to thermocapillary effect. This is confirmed by comparing the theoretically predicted terminal velocity of a pore in thermocapillary-induced motion[14] with experimentally observed velocity determined through micro-particle imaging velocimetry ($\mu$PIV). The theoretically predicted terminal velocity is given by[14]

$$v_{0,th} = \frac{\partial \sigma}{\partial T} \times \frac{R}{2\eta} \times \frac{dT}{dx}, \tag{1}$$

where $\frac{\partial \sigma}{\partial T}$ is the temperature gradient of surface tension, which for PDMS is 0.05 mN/(K m),[18,19] R is the bubble radius, and $\eta$ is the liquid medium viscosity (3.9 Pa s for PDMS). $\frac{dT}{dx}$ is the imposed temperature gradient, determined from the experimentally validated finite-element simulation model. Based on these values, the bubble terminal velocity in PDMS is found to be 21.4 $\mu$m/s. In contrast, $\mu$PIV measurements result in an experimentally measured velocity of 24.8 $\mu$m/s which is in reasonable agreement with the theoretical model.

Rayleigh number for the current experiments is found to be very small, around 2.6, which rules out natural convection of the bulk fluid as a possible reason for the motion of bubbles towards the hot microheater line.

The dynamics of the bubble rise through the PDMS matrix is governed by a balance between several competing phenomena. While the bubble moves laterally due to thermocapillary effect described above, it also moves up due to the net sum of buoyancy force acting upwards and inertial force and Stokes drag acting downwards. The thermocapillary force is not considered in the vertical direction since the microheater device produces a temperature gradient only in the horizontal direction while the PDMS membrane remains nearly isothermal in the vertical direction due to its small thickness relative to its width. Variation of temperature in the vertical direction predicted by the simulation model is plotted and is shown as a supplementary material. There is less than 1 °C temperature difference across the PDMS thickness. The Biot number[20] in the vertical direction, based on the PDMS thickness and thermal conductivity, and natural convection is found to be 0.04. The low value of Biot number further confirms vertical temperature homogeneity. Thus, force balance results in the following equation governing the bubble travel speed as a function of time:

$$\frac{dV}{dt} = g\left(\frac{\rho_{PDMS}}{\rho_{PEO}} - 1\right) - \frac{9\eta V(t)}{2R^2 \rho_{PEO}}, \tag{2}$$

where $V(t)$ is the vertical bubble speed, $R$ is the bubble radius determined from experiments, $g$ is the acceleration due to gravity, and $\rho$ and $\eta$ are PDMS density and viscosity, respectively obtained from literature.[21]

Equation (2) shows that pore formation and patterning involves trade-offs between multiple physical phenomena, including the viscosity increase due to the PDMS curing process, increased Stokes drag, higher rate of nucleation at higher temperature, lateral motion due to thermocapillary effect, etc. Note that while the bubble moves upwards, the PDMS around it continues to cure, resulting in a rapid increase in viscosity. While the cure extent of PDMS as a function of time at different temperatures is well-known,[21] not much work has been reported on PDMS viscosity as a function of cure extent. This is further complicated by the non-Newtonian nature of PDMS.[22] When this phenomenon occurs in the presence of a spatial temperature gradient due to the microheater line, gas bubbles are also attracted towards the hot region around the microheater due to thermocapillary effect, resulting in a spatially directed growth of pores. The bubbles reach stability once they reach the highest temperature region along the microheater line. The formation of a sustained pattern of pores depends on whether there is sufficient time for the pores to migrate to the microheater line before PDMS cures. At high microheater temperature, there is a greater thermocapillary force for migration, but lesser time before PDMS cures. At low microheater temperature, there is a weaker thermocapillary force but more available time for migration. This explains the four distinct experimentally observed temperature regimes of pore formation. The modeling of viscoelastic behavior of PDMS as a function of the curing process will further enhance the theoretical understanding of the observed phenomena.

This paper reports thermocapillary effect in PDMS, resulting in a method to produce self-assembled through-membrane pores in any desired pattern. Such patterned pores in PDMS may be useful for controlled cross-membrane species transport for bioanalysis, purification, etc. Experimentally measured pore migration speed is in good agreement with predicted value based on thermocapillary effect. Theoretical treatment presented in this work is expected to improve the understanding of coupled physics governing PDMS curing and gas migration within a curing PDMS matrix.

The authors gratefully acknowledge useful discussions with Dr. Samir Iqbal and Ms. Wintana Kahsai.

Microfabrication described in this work was carried out at Nanotechnology Research and Education Center at the University of Texas, Arlington. Part of this work was carried out with financial support from the Undergraduate Research Assistantship (URA) award from Honors College, University of Texas at Arlington.

[1]G. M. Whitesides, E. Ostuni, S. Takayama, X. Jiang, and D. E. Ingber, Annu. Rev. Biomed. Eng. **3**, 335 (2001).
[2]Y. Xia and G. M. Whitesides, Annu. Rev. Mater. Sci. **28**, 153 (1998).
[3]A. Khademhosseini, R. Langer, J. Borenstein, and J. P. Vacanti, Proc. Natl. Acad. Sci. U.S.A. **103**, 2480 (2006).
[4]R. Qi, Y. Wang, J. Li, C. Zhao, and S. Zhu, J. Membr. Sci. **280**, 545 (2006).
[5]S. Bose, T. Kuila, T. X. H. Nguyen, N. H. Kim, K.-t. Lau, and J. H. Lee, Prog. Polym. Sci. **36**, 813 (2011).
[6]H. J. Kim, S. S. Nah, and B. R. Min, Adv. Environ. Res. **6**, 255 (2002).
[7]J. C. McDonald, D. C. Duffy, J. R. Anderson, D. T. Chiu, H. Wu, O. J. A. Schueller, and G. M. Whitesides, Electrophoresis **21**, 27 (2000).
[8]J. Melin and S. R. Quake, Annu. Rev. Biophys. Biomol. Struct. **36**, 213 (2007).
[9]A. del Campo and C. Greiner, J. Micromech. Microeng. **17**, R81 (2007).
[10]W. T. Kahsai, U. H. T. Pham, J. S. Sankaran, and S. M. Iqbal, J. Appl. Phys. **112**, 024701 (2012).
[11]J. S. Sankaran, S. Goyal, W. T. Kahsai, U. H. T. Pham, and S. M. Iqbal, Adv. Sci. Lett. **4**, 3464 (2011).
[12]A. Javed, S. M. Iqbal, and A. Jain, Appl. Phys. Lett. **101**, 093707 (2012).
[13]A. Jain, K. D. Ness, and K. E. Goodson, Sens. Actuators B **143**, 286 (2009).
[14]N. O. Young, J. S. Goldstein, and M. J. Block, J. Fluid Mech. **6**, 350 (1959).
[15]See supplementary material at http://dx.doi.org/10.1063/1.4824444 for photolithography masks, microheater calibration curve, and a video showing the pore migration and alignment process.
[16]D. W. Berry, N. R. Heckenberg, and H. Rubinsztein-Dunlop, J. Mod. Opt. **47**, 1575 (2000).
[17]V. Y. Bazhenov, M. V. Vasnetsov, M. S. Soskin, and V. B. Taranenko, Appl. Phys. B **49**, 485 (1989).
[18]R. J. Roe, J. Phys. Chem. **72**, 2013 (1968).
[19]H. W. Fox, P. W. Taylor, and W. A. Zisman, Ind. Eng. Chem. **39**, 1401 (1947).
[20]F. P. Incropera and D. P. Dewitt, *Introduction to Heat Transfer*, 5th ed. (Wiley, Inc., New York, 2006).
[21]E. J. Wong, "Modeling and control of rapid curing in Polydimethylsiloxane (PDMS) for microfluidic device applications," Ph.D. thesis (Massachusetts Institute of Technology, 2010).
[22]F. Chambon and H. H. Winter, J. Rheol. **31**, 683 (1987).